Thermal and Near-Infrared Analyses of Central Uplifts of Martian Impact Craters. Cong Pan[1] and A. Deanne Rogers[1], [1]Stony Brook University, Department of Geosciences, 255 Earth and Space Science Building, Stony Brook, New York, 11794-2100, pancongggeosciences@gmail.com.

Introduction: Determining the mineralogy of a planetary surface and subsurface is important for understanding crustal evolution and alteration processes that occurred. Impact craters are natural probes into the subsurface. Particularly, the central uplift (CU) of an impact crater exposes rocks from the deep subsurface. We present a global spectral study of low-albedo CUs of Martian impact craters with diameter between 40-143 kilometers. By deriving mineral composition of central uplifts from MGS-TES data, comparing thermal infrared spectra between CUs and their surrounding regions, and detecting hydrated and iron-bearing minerals from CRISM, the bulk composition of subsurface and their alteration histories are investigated.

Data: We investigated TES data coverage of impact craters with central peaks or peak rings and diameter larger than 40 kilometer globally, using the crater database of [1]. This minimum diameter was chosen to locate craters whose CUs were large enough to be resolved in TES data. Within this set of craters, well-exposed and preserved CUs were prioritized using visible (THEMIS VIS, CTX, MOC and HiRISE) and daytime/nighttime THEMIS IR data. Thermal infrared spectra of CUs and their surrounding regions are from TES and THEMIS data. TES is also used to derive mineral abundance. High resolution CRISM data are used to search for secondary minerals (clay, sulfate and carbonate) and primary minerals (olivine and pyroxene).

Method: Our overall approach is as follows. First, we classified the craters based on average CU composition (TES-derived), to understand whether there are any clear trends in spatial distribution or vertical distribution (inferred from calculated maximum depth of excavation). Maximum depth of excavation of impact process d_e is estimated from crater diameter D_t based on Maxwell's Z-model of excavation flow fields [2]:

$$d_e \approx 0.1 D_t \quad (1).$$

Second, we conduct detailed analyses of spectral/mineralogic variability within each CU and their surroundings using TES, THEMIS and CRISM data. This allows for mineral identifications from smaller exposures that might be missed with larger averages.

A linear deconvolution method [3] is used to remove atmospheric components and derive mineral abundance using the libraries of atmosphere and minerals similar to [4]. Six groups of major minerals are derived for analysis: feldspar, olivine, sulfate, LCP: low-calcium pyroxene (orthopyroxene and pigeonite), HCP: high-calcium clinopyroxene (augite and diopside), and high-silica phases: combined modeled abundance of phyllosilicates, zeolites, opals and glasses.

The spectral angle mapper (SAM) algorithm [5], which measures spectral similarity between two spectra, is used to classify TES spectra of CUs. Unlike unsupervised clustering algorithm such as K-means treating each property in one observation with equal weight, SAM is a supervised algorithm calculating "angle" between two spectral observations, considering one observation is a vector in a N dimensional space, where N is the number of bands.

Result: There are 23 impact craters with quality TES data coverage and well preserved CUs, exposing crust depth at 4 to 14 kilometers (**Figure1**). They are classified to 8 classes: 13 craters in Class1, 4 craters in Class2 and 1 crater each in Class3 to Class8. Class3 to Class8 have lower signal to noise ratio than Class1 and Class2, because they contain less numbers of TES pixels and represent only a single orbit of TES data (figure2). Either signal to noise ratio or unique spectral features separates them to single crater classes. Both Class1 and Class2 are more representative of Surface Type 1 (ST1) than Type 2 (ST2). Class1 has lower abundance of feldspar and HCP, and higher abundance of olivine and high-silica phase comparing to Class2. For craters whose CUs are spectrally distinct from surroundings (using SAM criterion), most spectra of CUs have higher emissivity around 1100 cm^{-1} and lower around 900 cm^{-1} This is consistent with a higher abundance of mafic minerals in the CUs relative to surroundings.

An example for detailed comparison of CU and

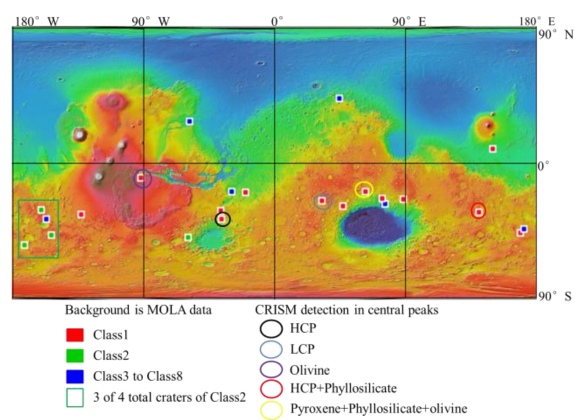

Figure1 (above). Distribution and preliminary classification of CUs surrounding region is an ~85km diameter crater located 199.75° E, -30.22° N (**Figure 2**). Hydration features are absent in CRISM images over this CU. TES spectra are selected from a single TES orbit, from the CU and from the crater ejecta (**Fig. 2A**). (Locating non-ejecta surfaces that might be representative of the "target" material is challenging. However, because the ejecta was still excavated from a shallower depth than the CU, it can be a useful comparison.) THEMIS DCS images (**Fig. 2B**) and surface emissivity spectra (**Fig. 2D**) indicate that the CU is spectrally distinct from surrounding regions, based on color differences in the DCS stretch and spectral shape. The surrounding region is similar to Surface Type 1 [7] for TES spectra, whereas the CU is different from Surface Type1 and Type2. Both the TES/THEMIS spectra and TES spectral models are consistent with LCP enrichment relative to the ejecta (LCP is used in highest abundance relative to other mineral groups in best fit TES models), consistent with relatively high CRISM LCP index values (>0.05) Elsewhere in the peak, smaller exposures (~100 m^2) of olivine are observed in CRISM data.

Discussion: Compositional variability in the subsurface could be expected for several scenarios, including a) differences between primary and secondary crust, b) fractionation of lavas during formation of secondary crust, c) sampling of ancient magma bodies intruded into the crust and crystallized at depth, and d) variation in subsurface alteration environments. As detailed information about mineral composition is obtained for the craters in our study, these potential scenarios will be evaluated for each crater.

Classification of the CU average compositions show no obvious spatial clusters, except that three of total four craters of Class2 are located in a region 186˚E, -28.5˚N~210˚E,-54˚N, which may indicate the subsurface in this region has a distinct bulk composition. We also observe no correlation with crater diameter, and therefore, excavation depth. These preliminary results based on average CU compositions, however, must be supplemented with detailed observations of each CU using TES, THEMIS and CRISM, because the quality of exposures varies within each CU.

The absence of hydrated minerals in CRISM images from our example CU suggests that the CU exposed relatively unaltered crustal materials from ~ 8 km depth. TES, THEMIS and CRISM data all indicate a compositional difference between deeper (~8km) and shallower (near-surface) crustal materials. The relatively LCP- and olivine-rich CU materials are consistent with compositions expected for shallow, secondary crust in thick-crust regions [8]. Future work will include comparison with other predicted compositions for crustal materials.

Future Work: We will expand our detailed analyses to craters 5-300km diameter and will interpret our CU mineral composition observations in light of crustal formation models based on detailed petrologic and geochemical analyses of martian meteorites and Gusev crater basalts [e.g. 8,9].

References: [1] Barlow N.J. et al. (2000) *JGR, 105(E11)*, 26733 [2] Maxwell D.E. (1977), *Impact & Explos. Crater., ed. Roddy D.J. et al,* 1003-1008. [3] Smith M. D. et al. (2000) *JGR, 105,* 9589-9607. [4] Rogers A. D. et al. (2007) *JGR, 112(E1),* E01003. [5] Kruse F. A. et al. (1993) *Rem Sens Env, 44,* 145-163. [6] Rogers A. D. et al. (2008) *Icarus, 200,* 446-462. [7] Bandfield J.L. (2000) *Science, 287,* 1626-1630.[8] McCubbin F.M. et. al (2008) *JGR, 113,* E11013 [9] Elkins-Tanton L. et al. (2005) *JGR, 110,* E12S01.

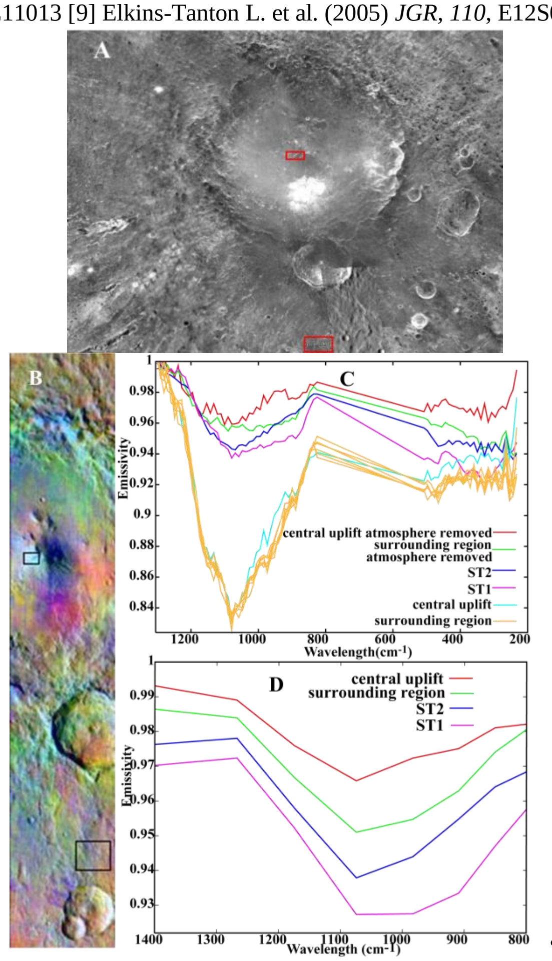

Figure 2. One example of detailed analysis of CU and surrounding region. A: TES data selection, background is THEMIS nighttime radiance; B: THEMIS DCS 8-7-5 and areas of spectral extraction for 2D.; C: TES spectra and atmosphere corrected spectra for CU and surroundings, compared to ST1 and ST2[7]; D: THEMIS atmosphere corrected spectra from CU and surroundings, compared to ST1 and ST2 [7].